

Orbital order in Mott insulators of spinless p-band fermions

Erhai Zhao and W. Vincent Liu

Department of Physics and Astronomy, University of Pittsburgh, Pittsburgh, Pennsylvania 15260, USA

A gas of strongly interacting spinless p-orbital fermionic atoms in 2D optical lattices is proposed and studied. Several interesting new features are found. In the Mott limit on a square lattice, the gas is found to be described effectively by an orbital exchange Hamiltonian equivalent to a pseudospin-1/2 XXZ model. For a triangular, honeycomb, or Kagome lattice, the orbital exchange is geometrically frustrated and described by a new quantum 120° model. We determine the orbital ordering on the Kagome lattice, and show how orbital wave fluctuations select ground states via the order by disorder mechanism for the honeycomb lattice. We discuss experimental signatures of various orbital ordering.

The electron orbital degree of freedom plays an important role in correlated quantum materials such as transition metal oxides [1]. Many intriguing phases observed in experiments are attributed to the coupling of electron d -orbitals, typically in the t_{2g} or e_g manifold, to the electron charge, spin, and/or the lattice degree of freedom [2, 3]. Understanding the intricate interplay between them remains a theoretical challenge. It is thus desirable to study simpler systems where the orbital degree of freedom is disentangled from others, namely “plain vanilla” orbital ordering in a Mott insulator.

Rapid advances in loading and controlling alkali atoms on the excited bands of optical lattices [4, 5, 6, 7] have made it possible to investigate orbital ordering of bosons and fermions in new settings [8, 9, 10, 11, 12, 13, 14]. Here we show that strongly interacting single species (spinless) p -orbital fermions on optical lattices can realize Mott states characterized by orbital-only models [15]. We consider the case where the degenerate p -orbitals of the optical potential well are partially occupied while the fully occupied s -orbital acts as “closed shell” and remain inert at low energy scales. Thus, these atomic Mott insulators differ significantly from their solid state counterparts of d electron systems in orbital symmetry. We derive the low energy effective orbital exchange Hamiltonian of p -band fermions in the strong coupling regime and commensurate filling for simple 2D lattices and determine their long range orbital ordering patterns.

Mott states of p -band fermions, described by orbital-only models, represent new examples of correlated states in condensed matter. Although we refer to the emergent low energy symmetry of the degenerate p -orbital states as pseudo-spin symmetry, it is not an internal symmetry like the true spin degree of freedom, but rather intrinsically spatial. As we shall demonstrate, in general $p_{x,y}$ orbital states transform as the components of a spinor under space rotation, in a manner reminiscent of the Lorentz spinor. This sets the orbital exchange models apart from the familiar spin exchange models.

Spinless lattice p-band fermions. We consider a gas of fermion atoms in a single hyperfine spin state loaded in an optical lattice interacting via a generic two-body po-

tential $\mathcal{V}(\mathbf{r}_1 - \mathbf{r}_2)$. Atoms interact predominately in the p -wave channel, i.e., in momentum space, $\mathcal{V}(\mathbf{k}' - \mathbf{k}) \simeq 3\mathcal{V}_1(k)(\hat{\mathbf{k}}' \cdot \hat{\mathbf{k}})$. The actual form of $\mathcal{V}_1(k)$ is unimportant for our discussion [16], as long as it reproduces the low energy p -wave scattering amplitude $f_1(k) = k^2/(-v_1^{-1} + c_1 k^2 - ik^3)$, where v_1 is the scattering volume and c_1 is the effective range parameter [17]. These parameters are known for ^{40}K [18]. For example, one can use a separable model potential [16] or a pseudopotential [19] with coupling constant $g_p = 12v_1\pi\hbar^2/m$ (m is the fermion mass). The strength of \mathcal{V}_1 can be tuned using a p -wave Feshbach resonance [20, 21, 22, 23]. We only consider repulsive interaction here.

We focus on a setup that captures the physics of the orbital symmetry and quantum degeneracy of fermionic atoms. We first consider a strongly anisotropic 3D cubic optical lattice potential, $V_{op}(\mathbf{r}) = \sum_{\mu=x,y,z} V_\mu \sin^2(k_L r_\mu)$ with $V_x = V_y$ and $V_z \gg V_{x,y}$, where k_L is the wavevector of the laser field and we set the lattice spacing to be unit, $a = \pi/k_L \equiv 1$. In the deep lattice limit, $V_\mu \gg E_R \equiv \hbar^2 k_L^2/2m$ (the recoil energy) for all three directions, the bottom of the optical potential at each lattice site can be approximated by a harmonic oscillator, and the lowest few energy levels are s, p_x, p_y, p_z orbital states. The $|p_x\rangle$ and $|p_y\rangle$ orbitals are degenerate, while $|s\rangle$ ($|p_z\rangle$) is well below (above) them, separated in energy by the harmonic oscillator frequencies $\hbar\omega_\mu = \sqrt{4V_\mu E_R}$. Due to the strong lattice potential in z -dimension, the system is dynamically separated into a stack of approximately independent layers with suppressed tunneling in between, each being two-dimensional (2D). Then, in order to explore the orbital-related quantum dynamics in such a lattice, one can fill fermions up to the p -band by having an average number of fermions per site between 1 and 2. In the atomic limit, for two particles per site, one of them occupies the s -orbital and the other one occupies either p_x or p_y . We shall refer to this as half filling.

We expand the fermion field operator in the Wannier basis, $\psi(\mathbf{r}) = \sum_{i,\ell} w_\ell(\mathbf{r} - \mathbf{R}_i) c_{i\ell}$, where \mathbf{R}_i is the lattice vector at site i in two dimensions and $\ell = s, p_x, p_y, p_z, \dots$ is the band index. Then the interacting system is described by a multi-band Hubbard model. Close to half

filling, with the filled s band and the empty p_z bands well separated from the degenerate p_x and p_y bands, the low energy effective model for the fermions is the following 2D p -band Hubbard Hamiltonian,

$$H_p = \sum_{i;\mu,\nu=x,y} t_{\mu\nu} [c_{i,\mu}^\dagger c_{i+\nu,\mu} + h.c.] + U \sum_i n_{ix} n_{iy}. \quad (1)$$

Here, $t_{\mu\nu} = t_{\parallel} \delta_{\mu\nu} + t_{\perp} (1 - \delta_{\mu,\nu})$ is the hopping amplitude of orbital μ in the ν direction [the orbitals will be denoted as $(p_x, p_y) \equiv (x, y) \equiv (\uparrow, \downarrow)$ interchangeably to lighten the notation], and U is the onsite repulsion between atoms in p_x and p_y orbital states. In the harmonic approximation of the Wannier function, the transverse hopping $t_{\perp} = -e^{-(\eta/2)^2} V_x/2$ is negative and small, while the longitudinal hopping $t_{\parallel} = (1 - \eta^2/2)t_{\perp}$ is positive and much larger in magnitude. Here, $\alpha_{\mu} = (V_{\mu}/E_R)^{1/4} k_L$ is the inverse of the harmonic oscillator length in the μ -dimension, and $\eta \equiv \alpha_x a$ is typically a large number. The onsite energy is given by $U = g_p \alpha_x^2 \alpha_z (22\alpha_x^2 + \alpha_z^2)/32(2\pi)^{3/2}$ in the pseudopotential approach. Eq.(1) looks like the ordinary one-band Hubbard model for spinless fermions, albeit with a twist: the p_x (pseudo-spin \uparrow) atoms prefer hopping in the x direction while the p_y (\downarrow) atoms prefer hopping in the y direction. Such anisotropy has dramatic consequences in the strong coupling limit.

Effective orbital exchange Hamiltonian. At half filling and in the strong coupling limit, $U \gg t_{\parallel}$, orbital fluctuation is the only remaining low energy degree of freedom. It is well known that virtual hopping processes lead to direct and higher order orbital exchange interactions [2]. In our case, as shown in Fig. 1, the nearest neighbor orbital exchange is strongly anisotropic as a direct consequence of the anisotropic shape of the p -orbitals. The effective Hamiltonian for H_p can be derived following the standard canonical transformation method. Up to order of t_{\parallel}^2 , it is given by $H^{(2)} = -U^{-1} T_{-1,1}^{(2)}$ in the notation of Ref. 24. We introduce pseudo-spin operator $T^+ = c_x^\dagger c_y$ and $T^z = (c_x^\dagger c_x - c_y^\dagger c_y)/2$, or equivalently $\mathbf{T} = \frac{1}{2} c_{\mu}^\dagger \boldsymbol{\sigma}_{\mu\nu} c_{\nu}$ in the Cartesian vector form with $\boldsymbol{\sigma}$ being the standard Pauli matrices, and rewrite $H^{(2)}$ as,

$$H_{\text{orb}} = \sum_{\langle i,j \rangle} [J_{xy} (T_i^+ T_j^- + h.c.) + J_z T_i^z T_j^z]. \quad (2)$$

Replacing \mathbf{T} with the usual spin \mathbf{S} in a magnetic system, Eq.(2) corresponds to the familiar XXZ model. The antiferro-orbital Ising exchange $J_z = 2(t_{\perp}^2 + t_{\parallel}^2)/U$ results from the longitudinal (and transverse) virtual exchange hopping. By contrast, the XY exchange $J_{xy} = 2t_{\perp} t_{\parallel}/U$ involves both longitudinal and transverse hopping, it is ferro-orbital ($J_{xy} < 0$) due to the opposite sign of t_{\parallel} and t_{\perp} . Because the transverse hopping amplitude of orbitals is small, we have $|J_{xy}| \ll |J_z|$, so the leading order interaction takes the form of antiferro-orbital Ising

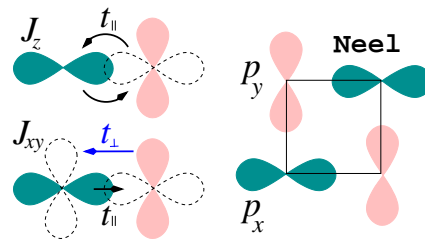


FIG. 1: (Color online) Left: Virtual hopping processes giving rise to the antiferro-orbital Ising exchange J_z and the ferro-orbital XY exchange J_{xy} . The transverse hopping t_{\perp} is much smaller than the longitudinal hopping t_{\parallel} and has opposite sign. Therefore $J_{xy} \ll J_z$. Dash lines indicate empty orbitals. Right: Neel orbital ordering on the square lattice.

model for pseudospin $T = \frac{1}{2}$,

$$H_{\text{orb}} \simeq J_z \sum_{\langle i,j \rangle} T_i^z T_j^z. \quad (3)$$

We neglect three body and ring exchange terms which are of higher order in t_{\parallel}/U . The Ising exchange favors antiparallel configuration of nearby pseudospins, i.e. perpendicular configuration of nearby p orbitals (one in p_x and the other p_y). Thus, the Mott state is antiferro-orbitally ordered on square lattice. The translational symmetry is broken with an alternative arrangement of p_x and p_y orbitals as shown in Fig. 1.

Frustrated 120° model on oblique lattices. We now generalize the analysis to oblique 2D lattices. For any vector e_{θ} directing at angle θ with the x axis, such as the bond direction indicated in Fig. 2, it is convenient to introduce a local coordinate system with axis \tilde{x} and \tilde{y} rotated from the global coordinate system by θ . The p -orbital wave functions transform under rotation as the components of a planar vector, i.e.,

$$\begin{aligned} c_x &\rightarrow \tilde{c}_x = c_x \cos \theta + c_y \sin \theta, \\ c_y &\rightarrow \tilde{c}_y = -c_x \sin \theta + c_y \cos \theta. \end{aligned} \quad (4)$$

Accordingly, the pseudospin operators transform as

$$\begin{aligned} T_z &\rightarrow \tilde{T}_z = T_x \sin 2\theta + T_z \cos 2\theta, \\ T_x &\rightarrow \tilde{T}_x = T_x \cos 2\theta - T_z \sin 2\theta, \\ T_y &\rightarrow \tilde{T}_y = T_y. \end{aligned} \quad (5)$$

In other words, the pseudospin vector \mathbf{T} is rotated by 2θ about the y axis in the pseudospin space. The leading order exchange interaction between site i and j , connected by bond e_{θ} , is then given by $J_z \tilde{T}_i^z \tilde{T}_j^z$. Note the value of longitudinal hopping along e_{θ} , and consequently J_z , for a specific lattice depends on details of the optical potential.

We are particularly interested in the triangular and honeycomb lattice, both of which can be implemented using interfering laser beams. For these lattices (lattice spacing $a = 1$), we introduce three basis vectors: $\hat{e}_1 \equiv \hat{x}$,

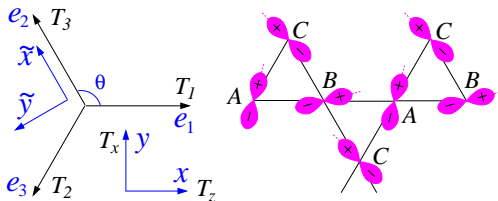


FIG. 2: (Color online) Left: The spatial coordinate system (in blue). Basis vectors e_j are at 120° from each other. Three pseudospins T_j (in black) defined on bond e_j . The quantization axis T_z is x (p_x). Right: Orbital ordering on an individual triangle ABC and long range order on the kagome lattice.

\hat{e}_2 , and \hat{e}_3 , which are 120° from each other as shown in Fig. 2 and use T_j to denote the operator \hat{T}_z along bond e_j ($j = 1, 2, 3$). Explicitly, $T_1 = T_z$, $T_2 = -\frac{1}{2}T_z - \frac{\sqrt{3}}{2}T_x$, and $T_3 = -\frac{1}{2}T_z + \frac{\sqrt{3}}{2}T_x$, all lying within the xz plane. Then the orbital exchange Hamiltonian can be put into a simple form,

$$H_{120} = J_z \sum_{\mathbf{R}, j} T_j(\mathbf{R}) T_j(\mathbf{R} + \hat{e}_j), \quad (6)$$

where the sum over \mathbf{R} includes all lattice sites (or the sites within the A sublattice) for the triangular (or honeycomb) lattice. We call Eq. (6) the quantum 120° model, as a formally similar Hamiltonian was proposed to describe the two-fold degenerate e_g electrons in cubic perovskites [15, 25, 26, 27]. The underlying physics is however very different. There, e_j label the cartesian basis vectors of the *cubic* lattice, while the 120° configuration of three T_j 's arises from a fundamentally different transformation property of two d -orbitals, $|3z^2 - r^2\rangle$ and $|x^2 - y^2\rangle$, under the permutation of x, y, z .

The antiferro-orbital exchange favors perpendicular alignments of nearest neighbor orbitals along bonds. Apparently, it is impossible to achieve this for all three bonds on an elementary triangle. Nor is it possible for three bonds joining at a site on the honeycomb lattice. The orbital exchange is thus geometrically frustrated on the triangular and honeycomb lattice. By frustration, we mean the energy on each bond cannot be minimized simultaneously [28]. As we shall show below, the classical ground state possesses a continuous degeneracy for the honeycomb lattice. Solving the quantum 120° model is a nontrivial task, e.g., it remains an open problem even for the cubic lattice [15, 25, 26, 27, 29]. Here, in searching for the ground state ordering pattern, we employ the semiclassical analysis which proves fruitful in the study of frustrated magnets [30]: first find the classical ground state, then consider the effect of leading order orbital wave fluctuations. Formally, this is done by generalize H_{120} to arbitrary pseudospin $T \geq \frac{1}{2}$ and consider the limit of large T .

First we determine the classical ground state of H_{120} on a triangle cluster shown in Fig. 2. We parametrize the

pseudospins at vertex A, B, C with angles $\phi_{A,B,C}$ with respect to the T_z axis (AB bond). The classical energy, $E/T^2 = f(0; A, B) + f(2\pi/3; A, C) + f(4\pi/3; B, C)$ where $f(\gamma; A, B) \equiv \cos(\gamma - \phi_A) \cos(\gamma - \phi_B)$, is minimized when $\phi_A - \phi_B = \phi_C - \phi_A = 2\pi/3$, $\phi_A = 5\pi/6$ or $11\pi/6$. The two energy minima manifest the C_2 symmetry of H_{120} , which is invariant under a π -rotation of \mathbf{T} about the y axis, i.e. $T_{x,z} \rightarrow -T_{x,z}$ with $\theta = \pi/2$ in (5). The corresponding orbital configuration is shown in Fig. 2, where the orbital at A forms angle $\phi_A/2 = 75^\circ$ with the AB bond. Permutation of (A, B, C) yields configurations of the same energy. This result immediately tells us the classical orbital ordering pattern (see Fig. 2) on the Kagome lattice, which consists of corner sharing triangles.

Orbital order by disorder. For the bipartite honeycomb lattice, we introduce transformation $T_{x,z} \rightarrow \bar{T}_{x,z} = \pm T_{x,z}$, with $+$ ($-$) for sites within the A (B) sublattice. Then the orbital exchange become ferro-orbital in terms of the new $\bar{\mathbf{T}}$ operators, $H_{120} = -J_z \sum_{\mathbf{R} \in A, j} \bar{T}_j(\mathbf{R}) \bar{T}_j(\mathbf{R} + \hat{e}_j)$. It can be rewritten (apart from a constant factor) as

$$\bar{H}_{120} = \frac{J_z}{2} \sum_{\mathbf{R} \in A, j} [\bar{T}_j(\mathbf{R}) - \bar{T}_j(\mathbf{R} + \hat{e}_j)]^2, \quad j = 1, 2, 3. \quad (7)$$

Therefore, the classical energy is minimized for any homogeneous configuration $(\bar{T}^z, \bar{T}^x)(\mathbf{R}) = (T \cos \phi, T \sin \phi)$, independent of the polar angle ϕ . This implies Neel (antiferro) orbital ordering. Note that this continuous $SO(2)$ degenerate manifold of classical ground states is not an inherent property of H_{120} which is only invariant under finite point group rotations. Orbital wave excitations are important quantum fluctuations beyond mean field theory. To the leading order in $1/T$, their correction to the ground state energy can be computed following the spirit of Holstein-Primakov spin wave theory [30]. The algebra is cumbersome but straightforward. The central result is the quantum correction to the ground state energy per unit cell (containing one A site and one B site),

$$\frac{E_c(\phi)}{TJ_z} = \frac{1}{N} \sum_{\mathbf{k}, \lambda} \omega_\lambda(\mathbf{k}) - \frac{3}{2}. \quad (8)$$

Here, index $\lambda = \pm 1$ labels the two branches of the orbital wave excitations with dispersion $\omega_\lambda(\mathbf{k}) = (\sqrt{3}/4)\sqrt{3 + 2\lambda|\beta_{\mathbf{k}}(\phi)|}$. The form factor $\beta_{\mathbf{k}}(\phi) = \sin^2(\phi)e^{i\mathbf{k} \cdot \hat{e}_1} + \sin^2(\phi - \pi/3)e^{i\mathbf{k} \cdot \hat{e}_2} + \sin^2(\phi + \pi/3)e^{i\mathbf{k} \cdot \hat{e}_3}$. N is the number of sites within the A sublattice, and the \mathbf{k} sum is within the first Brillouin zone of the triangular sublattice. $E_c(\phi)$ is plotted in the right panel of Fig. 3 for $\phi = 0$ to π , and $E_c(\phi + \pi) = E_c(\phi)$. We see that orbital fluctuation lifts the $SO(2)$ degeneracy and chooses ground state $\phi_n = n\pi/3$ (n is any integer), where function $E_c(\phi)$ reaches minimum. This mechanism is well known in frustrated spin systems as ‘‘order by disorder’’

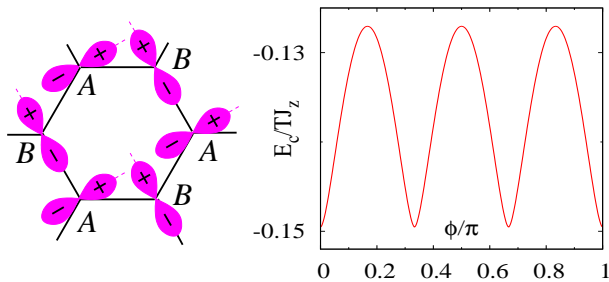


FIG. 3: (Color online) Left: Neel orbital ordering on the honeycomb lattice. The orbital at site A forms an angle of 30° with the horizontal AB bond. Global rotation of all orbitals by $n\pi/6$ yields degenerate configurations. Right: The quantum fluctuation correction to the ground state energy per unit cell, E_c/TJ_z , which reaches minima at $\phi_n = n\pi/3$. This lifts the continuous degeneracy of the classical ground states.

[28, 30]. The Left panel of Fig. 3 shows a representative orbital ordering pattern corresponding to $n = 1$, i.e., the p -orbital at site A is at angle $\phi_{n=1}/2 = 30^\circ$ with the horizontal AB bond. Successive global rotation of all orbitals by $\pi/6$ yields degenerate Neel configurations.

Finally we turn to the triangular lattice. We limit ourselves to 3-sublattice (R3) ordering [30] as one of the potential orders for pseudospin $T = 1/2$ [31]. The R3 order is parametrized by three polar angles, $\phi_{A,B,C}$, describing the in-plane pseudospins at each sublattice A, B, C . The classical energy per unit cell $E/T^2 = 3[\cos(\epsilon_1) + \cos(\epsilon_2) + \cos(\epsilon_1 + \epsilon_2)]/2$ only depends on two independent parameters $\epsilon_1 = \phi_A - \phi_B$ and $\epsilon_2 = \phi_B - \phi_C$, and it is minimized for $\epsilon_1 = \epsilon_2 = \pm 2\pi/3$. Therefore, the classical R3 configuration is infinitely degenerate with its degeneracy parametrized by ϕ_A . Its orbital wave analysis will be presented elsewhere.

To summarize, our mean-field and low energy fluctuation analysis suggests new correlated Mott phases with long range p -orbital ordering on the kagome, honeycomb, and triangular lattice. At finite temperature, we expect thermal fluctuations stabilize orbital ordering, as previously demonstrated for the cubic 120° model [15, 29]. Our analysis is very suggestive but cannot be taken as complete for pseudospin $T = 1/2$. There, quantum fluctuation may be strong enough to melt the long range orbital order, raising the possibility of realizing a disordered “orbital liquid” ground state. Future work is needed to address this open question.

Detecting the orbital order. Here, we predict experimental signatures of the orbital-ordered phases found above in the density-density (noise) correlation function, $G(\mathbf{r}, \mathbf{r}'; t) = \langle n(\mathbf{r}, t)n(\mathbf{r}', t) \rangle - \langle n(\mathbf{r}, t) \rangle \langle n(\mathbf{r}', t) \rangle$, which can be measured in the time of flight image taken after time t . We generalize the analysis of Ref. [10, 32, 33] to the case of multi-orbital spinless fermions and focus on various contributions from $\langle c_{\mathbf{q},\mu}^\dagger c_{\mathbf{q},\nu} c_{\mathbf{q}',\mu'}^\dagger c_{\mathbf{q}',\nu'} \rangle$.

Here $\mathbf{q} = m\mathbf{r}/\hbar t + \mathbf{G}$ is the quasimomentum folded into the first Brillouin zone of the underlying lattice, \mathbf{G} is the reciprocal wave vector, and μ, ν are the orbital indices. The closed-shell s -fermions contribute the usual anti-bunching dips at \mathbf{G} , reflecting the Fermi statistics [32, 34]. The p -fermions on the other hand contribute additional terms such as structure factor $\langle T_{\mathbf{q}}^z T_{\mathbf{q}'}^z \rangle$ and $\langle T_{\mathbf{q}}^+ T_{\mathbf{q}'}^- \rangle$, which lead to new dips at \mathbf{G}_r , the reciprocal lattice wave vector of the enlarged unit cell in the ordered state. For example, $\mathbf{G}_r = (\pi, \pi), (0, \pi), (2\pi/\sqrt{3}, 0)$, for the square, kagome, and honeycomb lattice, respectively.

Note Added. After the submission of our manuscript, there appeared Ref. [35] which independently proposed and studied a similar quantum 120° model.

We thank C. Ho and V. Stojanovic for helpful discussions. This work is supported in part by ARO W911NF-07-1-0293.

-
- [1] Y. Tokura and N. Nagaosa, *Science* **288**, 462 (2000).
 - [2] K. I. Kugel and D. I. Khomskii, *Sov. Phys. Usp.* **25**, 231 (1982).
 - [3] G. Khaliullin, *Prog. Theor. Phys. Suppl.* **160**, 155 (2005).
 - [4] M. Köhl, H. Moritz, T. Stöferle, K. Günter, and T. Esslinger, *Phys. Rev. Lett.* **94**, 080403 (2005).
 - [5] A. Browaeys et al, *Phys. Rev. A* **72**, 053605 (2005).
 - [6] T. Mueller, S. Foelling, A. Widera, and I. Bloch, *arXiv:0704.2856*.
 - [7] M. Anderlini et al., *Nature* **448**, 452 (2007).
 - [8] A. Isacsson and S. M. Girvin, *Phys. Rev. A* **72**, 053604 (2005).
 - [9] A. B. Kuklov, *Phys. Rev. Lett.* **97**, 110405 (2006).
 - [10] W. V. Liu and C. Wu, *Phys. Rev. A* **74**, 013607 (2006).
 - [11] C. Wu, W. V. Liu, J. Moore, and S. Das Sarma, *Phys. Rev. Lett.* **97**, 190406 (2006).
 - [12] C. Wu, D. Bergman, L. Balents, and S. D. Sarma, *Phys. Rev. Lett.* **99**, 070401 (2007).
 - [13] K. Wu and H. Zhai, *arXiv:0710.3852*.
 - [14] C. Wu and S. Das Sarma, *arXiv:0712.4284*.
 - [15] J. van den Brink, *New J. Phys.* **6**, 201 (2004).
 - [16] T.-L. Ho and R. B. Diener, *Phys. Rev. Lett.* **94**, 090402 (2005).
 - [17] V. Gurarie and L. Radzihovsky, *Ann. of Phys.* **322**, 2 (2007).
 - [18] C. Ticknor, C. A. Regal, D. S. Jin, and J. L. Bohn, *Phys. Rev. A* **69**, 042712 (2004).
 - [19] L. Pricoupenko, *Phys. Rev. Lett.* **96**, 050401 (2006).
 - [20] C. A. Regal, C. Ticknor, J. L. Bohn, and D. S. Jin, *Phys. Rev. Lett.* **90**, 053201 (2003).
 - [21] K. Günter, T. Stöferle, H. Moritz, M. Köhl, and T. Esslinger, *Phys. Rev. Lett.* **95**, 230401 (2005).
 - [22] J. Zhang et al, *Phys. Rev. A* **70**, 030702 (2004).
 - [23] C. H. Schunck et al, *Phys. Rev. A* **71**, 045601 (2005).
 - [24] A. H. MacDonald, S. M. Girvin, and D. Yoshioka, *Phys. Rev. B* **37**, 9753 (1988).
 - [25] J. van den Brink, P. Horsch, F. Mack, and A. M. Oles, *Phys. Rev. B* **59**, 6795 (1999).
 - [26] M. V. Mostovoy and D. I. Khomskii, *Phys. Rev. Lett* **89**, 227203 (2002).

- [27] W.-L. You, G.-S. Tian, and H.-Q. Lin, Phys. Rev. B **75**, 195118 (2007).
- [28] H. T. Diep, *Frustrated Spin Systems* (World Scientific, 2004).
- [29] Z. Nussinov, M. Biskup, L. Chayes, and J. van den Brink, Europhys. Lett. **67**, 990 (2004).
- [30] G. Murthy, D. Arovas, and A. Auerbach, Phys. Rev. B **55**, 3104 (1997).
- [31] An independent work of Wu [35] suggests that the classical H_{120} model develops strip order on the triangular lattice, which is in a different symmetry class than we considered.
- [32] E. Altman, E. Demler, and M. D. Lukin, Phys. Rev. A **70**, 013603 (2004).
- [33] A. F. Ho, Phys. Rev. A **73**, 061601 (2006).
- [34] T. Rom et al, Nature **444**, 733 (2006).
- [35] C. Wu, arXiv:0801.0888.